



Characterization of NiO/CoPc nanocomposite material synthesized by solvent evaporation route

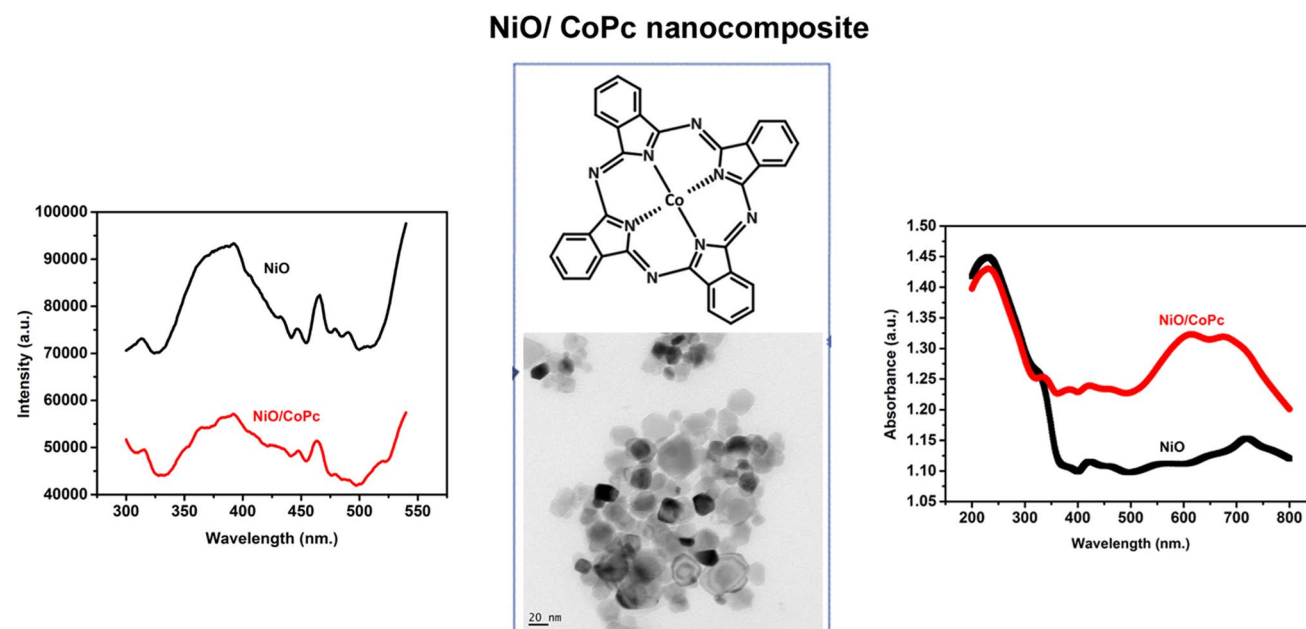
P. A. Sheena^{1,2} · K. P. Priyanka³ · A. Sreedevi³ · Thomas Varghese³

Received: 22 May 2018 / Accepted: 25 June 2018 / Published online: 29 June 2018
© The Author(s) 2018

Abstract

Nickel oxide/cobalt phthalocyanine (NiO–CoPc) nanocomposite is synthesized by solvent evaporation method. The synthesized nanocomposite is characterized for thermal, structural, and optical properties. Thermogravimetric and differential thermal analysis results proved the thermal stability of the sample. XRD patterns revealed an average crystallite size of 16 and 17.5 nm, respectively, for the pure and nanocomposite samples. The formation of NiO/CoPc nanocomposite is confirmed by the FTIR results. The characteristic B and Q bands of metal phthalocyanines are visible in the absorption spectrum. A decrease in band gap and an enhanced absorption in the visible region are observed for the nanocomposite. The PL emission spectrum of the nanocomposite exhibits fluorescence quenching which makes them suitable for solar cells and photocatalysis. This work constitutes the first report on the synthesis and characterization of the NiO/CoPc nanocomposite.

Graphical abstract



Keywords NiO/CoPc nanocomposite · Solvent evaporation · UV–visible absorption · Photoluminescence

✉ Thomas Varghese
nanoncm@gmail.com

Extended author information available on the last page of the article

Introduction

Nanocomposites are materials of considerable interest because of their unique design and excellent properties. The combination of organic/inorganic nanocomposites has attracted much attention because of the blending of their distinct physical and chemical properties. There are a rich variety of possible combinations of organic–inorganic materials. Organic materials offer interesting optical properties, structural flexibility, tunable electronic properties and the potential for semiconducting behaviour [1]. Phthalocyanines are p-type organic semiconductors with high stability, having wide range of applications from medicine to microelectronics [2]. Out of these; metal phthalocyanines (M.Pc) have invited attention due to their good thermal and chemical stability, photoconductivity and semi-conducting nature. Their thermal and chemical stability are important properties that make them suitable for electrochemical sensors [3]. The properties of M.Pcs are determined by the conjugated π electron ring system of the molecule. Due to their high electron transfer abilities, M.Pcs are promising candidates in the field of molecular electronics, optoelectronics, etc. The potential applications of M.Pcs include solar energy conversion [4], photo detectors [5, 6], chemical sensors [7], gas sensors [8] and nonlinear optics [9]. In the other hand, inorganic metal nanoparticles exhibit good thermal and mechanical stability, high carrier mobility, and varied magnetic and dielectric properties [1].

Pure single crystalline NiO is identified as a Mott–Hubbard insulator having very low conductivity at ordinary temperatures. It is reported that the presence of Ni^{2+} vacancies makes nanosized NiO a wide band gap p-type semiconductor [10]. The structural and optical properties of NiO can be finely tuned with the incorporation of CoPc into the NiO lattice. In the present work, solvent evaporation method is employed to synthesize NiO/CoPc nanocomposite. The thermal, structural and optical properties of the nanocomposite are studied and compared with that of NiO nanoparticles. This is the first report on the synthesis and characterization of NiO/CoPc nanocomposites. However, literatures are available on the study of other metal oxide/CoPc nanocomposites. Priyanka et al. have reported the improved visible light photocatalytic degradation of organic dyes using TiO_2/CoPc nanocomposite [11]. CoPc-loaded nanotitania is used for the photocatalytic reduction of carbon dioxide as reported by Liu et al. [12]. Babitha et al. have observed a reduction in band gap for CeO_2/CoPc nanocomposite synthesized by solvent evaporation method [13].

Experimental details

Materials

All the chemicals used for the synthesis are of analytical grade. Nickel nitrate hexahydrate [$\text{Ni}(\text{NO}_3)_2 \cdot 6\text{H}_2\text{O}$, 99.8%, Merck], ammonium carbonate [$(\text{NH}_4)_2\text{CO}_3$, 99.9%, Merck], cobalt phthalocyanine (CoPc, Sigma Aldrich), dimethyl formamide, dimethyl sulphoxide and ethanol (Merck) are used for the synthesis of the nanocomposite. Distilled water is used for the synthesis.

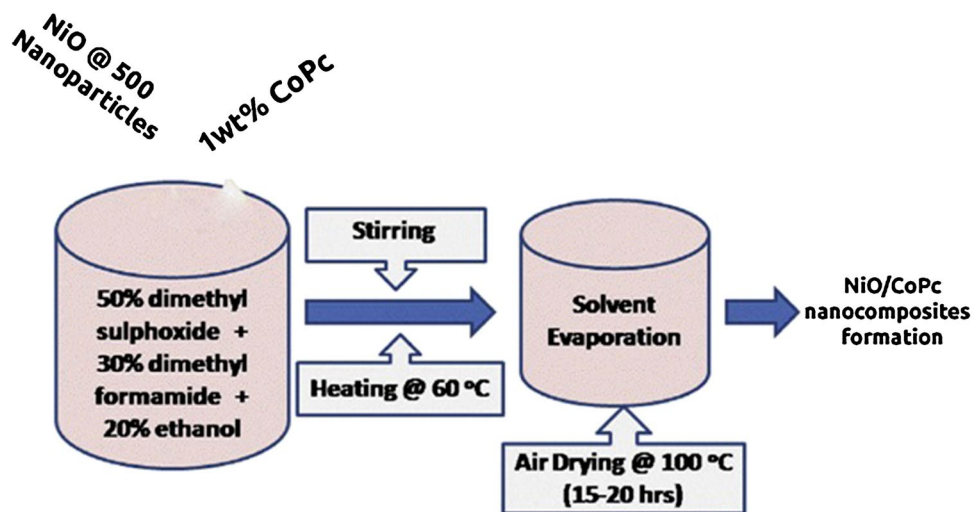
Synthesis of NiO–CoPc nanocomposite

The NiO–CoPc nanocomposite is prepared by solvent evaporation method. A solvent mixture containing 50% dimethyl sulphoxide, 30% dimethyl formamide and 20% ethanol is prepared. 1 wt% cobalt phthalocyanine is dissolved in the mixture under constant magnetic stirring and simultaneous heating at 50 °C. NiO nanoparticles prepared by chemical precipitation method and calcined at 500 °C are gradually added to this solution. The procedure adopted for the synthesis of NiO nanoparticles is reported elsewhere [14]. After complete evaporation of the solvent mixture, the obtained material is washed several times to remove remaining organic solvents and dried at 100 °C in a hot air oven for 18 h. The scheme for the synthesis is shown in Fig. 1.

Characterization

The thermal behaviour of the NiO/CoPc nanocomposite from room temperature to 880 °C is studied by thermogravimetric analysis (TGA) and differential thermal analysis (DTA) using Perkin Elmer STA 6000, at a heating rate of 20 °C min^{-1} . The structural characterization is done by PXRD method using Bruker D8 Advance X-ray diffractometer ($\lambda = 1.5406 \text{ \AA}$, step size = 0.020° and step time = 32.8 s) with $\text{CuK}\alpha$ radiation ($\lambda = 1.5406 \text{ \AA}$, X-ray tube voltage = 40 kV and current = 35 mA) from 0 to 90 °C. TEM and HRTEM images are recorded at an accelerating voltage of 200 kV on a Jeol/JEM 2100 instrument. Thermo Nicolet, Avatar 370 instrument is used to record Fourier transform infrared spectra of the samples in the range 4000–400 cm^{-1} . The optical absorption spectra of the samples are recorded using Shimadzu 2600/2700 UV–visible spectrophotometer in the wavelength range of 200–800 nm. PL spectra of the samples at room temperature are measured using a Fluoromax 3 spectrophotometer.

Fig. 1 Scheme of synthesis of NiO/CoPc nanocomposite



Results and discussion

Thermogravimetric analysis

TG/DTG curves of the prepared precursor and NiO/CoPc nanocomposite are displayed in Fig. 2. The precursor decomposed completely at around 350 °C to form nickel oxide. A small weight loss of about 6% is observed in the TG curve of the composite which confirms its thermal stability. The weight loss up to 400 °C is related to the evaporation of trapped solvents such as water and ethanol. It is reported that CoPc is stable up to about 400 °C and decomposition starts around 425 °C [15]. This may be the reason for a comparatively sharp weight loss (1%) around 400 °C, which occurs by the partial decomposition of macrocyclic structure which results in the loss of low weight atoms from the composite structure [16].

The DTG curve of the sample shows an endothermic peak around 60 °C. This represents a weight loss due to the

combustion of organic residues. A sharp endothermic peak positioned around 428 °C also indicates a change of weight suggesting the oxidative degradation of the sample. Thermal analysis confirms the thermal stability of the nanocomposite in the temperature range.

XRD analysis

The structure, composition and purity of the prepared samples are analysed using XRD. Figure 3 shows the X-ray diffraction patterns of NiO and NiO/CoPc samples. The sharpness of diffraction peaks indicates the crystallinity of the sample. The observed peak positions at 2θ values 37.424, 43.463, 63.030, 75.554, and 79.53 °C are indexed as (111), (200), (220), (311), and (222) crystal planes of NiO, respectively (space group: Fm3m), with lattice constant $a = 4.161 \text{ \AA}$ (JCPDS card No. 73-1519). Due to the low concentration of CoPc, no peaks of phthalocyanine are observed in the diffraction pattern. However, all the

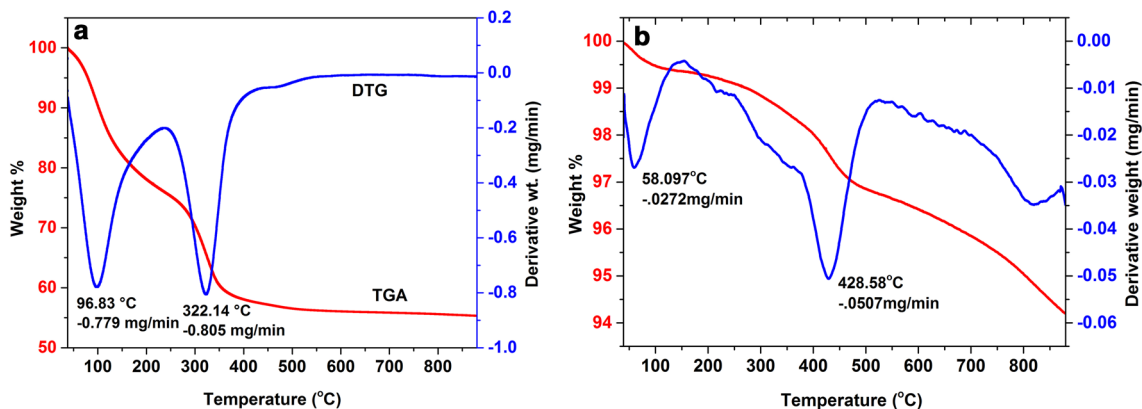


Fig. 2 TGA/DTG curves of **a** NiO and **b** NiO/CoPc nanocomposite



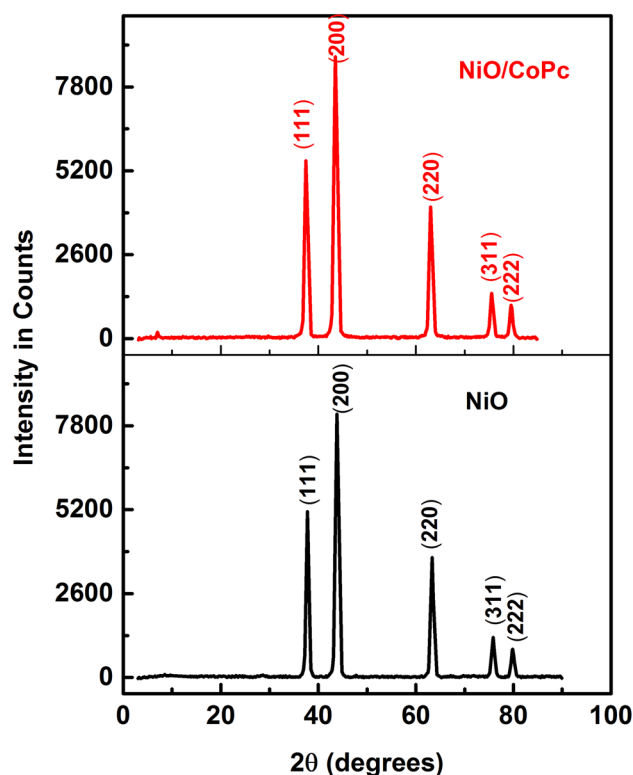


Fig. 3 XRD spectra of NiO and NiO/CoPc nanocomposite

Table 1 Geometric parameters of NiO and NiO/CoPc from XRD spectra

Sample	Crystallite size (nm)		Micro-strain
	Scherrer equation	<i>W-H</i> analysis	
NiO	16	18.5	6.656×10^{-4}
NiO/CoPc	17.5	21.1	7.259×10^{-4}

prominent peaks are shifted slightly to lower angle side for the nanocomposite.

The structural parameters of NiO/CoPc nanocomposite are compared with that of pure NiO in Table 1. The average crystallite size of NiO and NiO/CoPc samples obtained using Scherrer equation, $D = k\lambda/\beta\cos\theta$ [17] are 16 and 17.5 nm, respectively. The increase in crystallite size and interplanar spacing for the composite shows the growth of unit cell with the inclusion of phthalocyanine.

The size and micro-strain contributions to the broadening of XRD peaks is calculated by Williamson–Hall equation, $\beta\cos\theta = k\lambda/D + 4\epsilon\sin\theta$ [18]. The micro-strain values for NiO and NiO/CoPc are 6.656×10^{-4} and 7.259×10^{-4} , respectively. The presence of oxygen vacancies, dislocations and crystal imperfections may contribute to the micro-strain. The defect centres formed due to the

insertion of CoPc into the NiO lattice are responsible for the increase in micro-strain.

TEM analysis

To reveal the morphology and size of the synthesized particles, TEM images of pure NiO and the nanocomposite are recorded as displayed in Fig. 4. The particle size of the composite material ranges from 20 to 25 nm. The bright field image of the composite shows the cube-like shape of the particles which are well-dispersed with smooth surfaces. The crystallinity of the sample is confirmed by the bright spots in the SAED pattern. The particle size distribution of NiO/CoPc nanocomposite is plotted in the histogram in Fig. 5.

FTIR analysis

FTIR spectra of pure and nanocomposite samples are presented in Fig. 6a. The spectrum of the nanocomposite shows some prominent peaks which confirm the presence of CoPc. Table 2 presents the observed modes in NiO and NiO/CoPc, along with the reported values for CoPc.

The intense peak observed in both samples at 412 cm^{-1} is due to Ni–O stretching vibration. The broad band centred at 3430 cm^{-1} is assigned to O–H stretching vibrations and the band at 1625 cm^{-1} is attributed to H–O–H bending vibration mode [19, 20]. Figure 6b shows FTIR spectrum of the nanocomposite in the range $1500\text{--}700\text{ cm}^{-1}$. The bands at 723 (C–H out of plane deformation), 918 (metal ligand vibration), 1112 (C–H in plane bending), 1156 (C–N in plane bending), 1287 (C–N stretching) and 1330 cm^{-1} (C–C stretching) confirm the existence of CoPc in the composite [21]. The band located at 723 cm^{-1} in NiO/CoPc represents the characteristic α -phase of CoPc [13].

UV–visible studies

Figure 7 shows the UV–visible absorption spectra of NiO and NiO/CoPc composite in the range 200–800 nm.

A strong absorption in the range 200–300 nm centred at 235 nm is observed in both samples, which are attributed to band gap absorption in NiO [22]. The absorption peak of NiO arises from the transition between 2p states of oxygen in the top of the valence band and 3d states of Ni at the bottom of the conduction band [23].

Compared to NiO, NiO/CoPc shows very good absorption in the range 300–750 nm. This corresponds to the B band (Sorret band) and Q band which are characteristic of metal phthalocyanines. This indicates the successful incorporation of CoPc in NiO. Both these bands arise from $\pi\text{--}\pi^*$ transitions of the conjugated macrocycle of 18 π -electrons [24, 25]. The two absorption peaks in the Q band are at 2.02 and 1.83 eV. The higher-energy peak (Q1) has a slightly

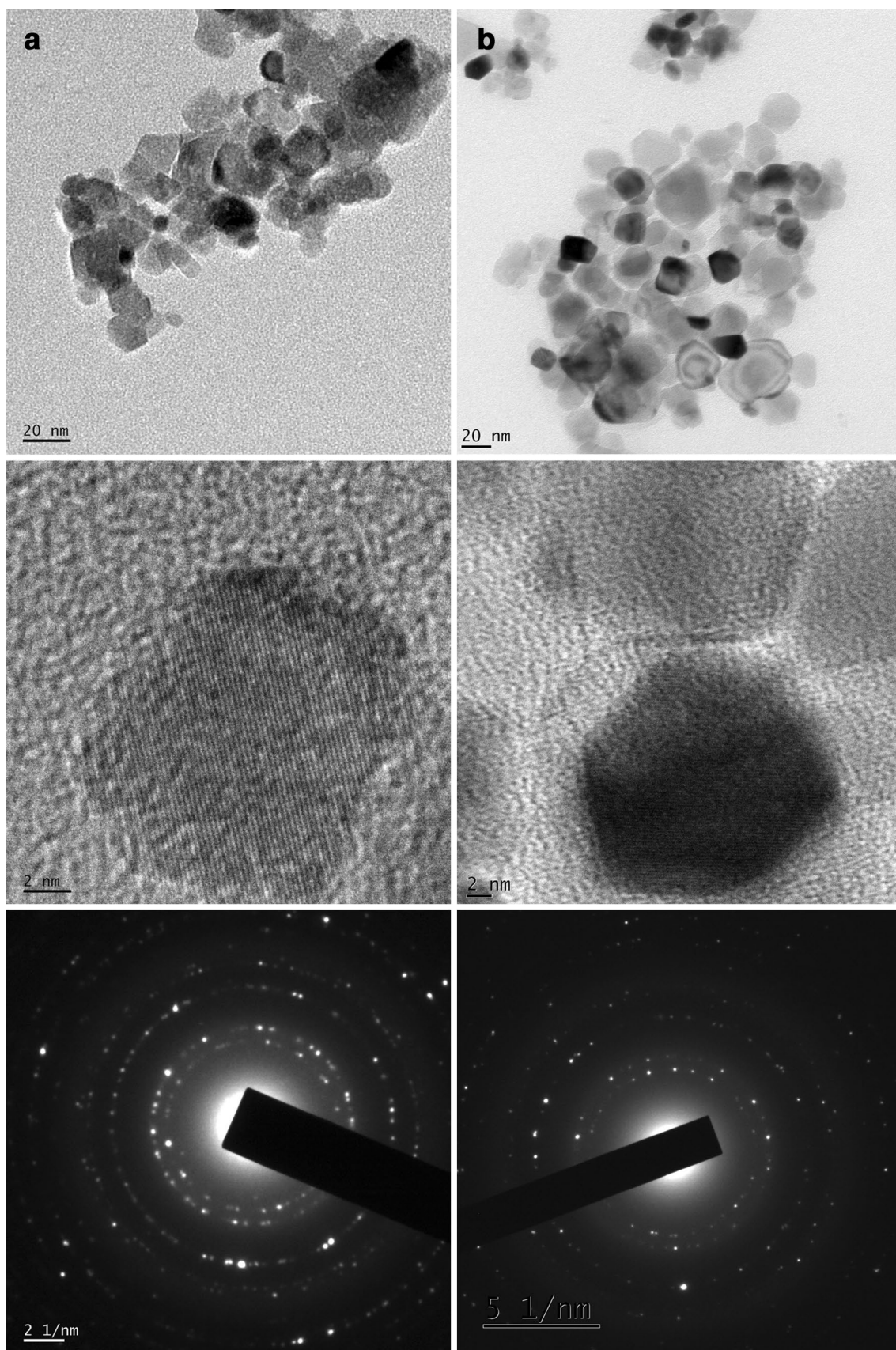


Fig. 4 TEM images of NiO and NiO/CoPc nanocomposite

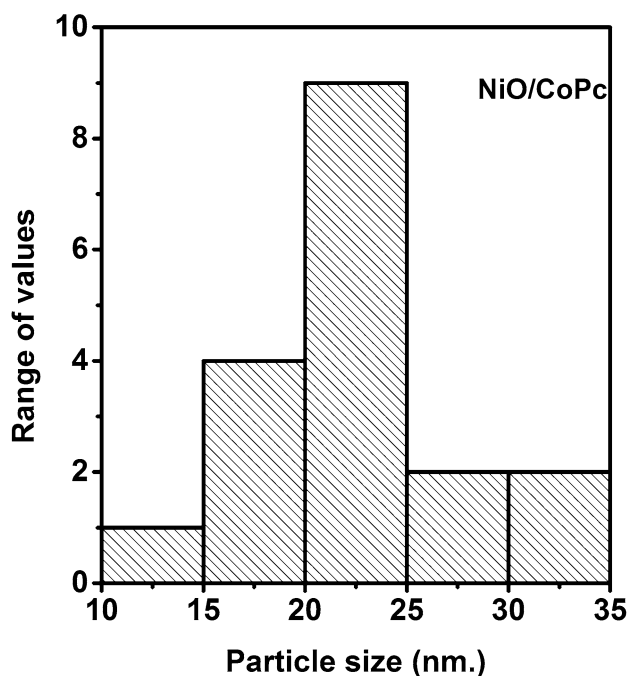


Fig. 5 Size distribution of NiO/CoPc nanocomposite

larger intensity compared to the second peak (Q2), which is a typical feature of CoPc α -phase [26]. The electrons in the π orbital which overlap between molecules are responsible for the absorption spectra [27].

The plot of $h\nu$ vs. $(ah\nu)^2$ for the pure sample and the nanocomposite are displayed in Fig. 8. The intrinsic band gap energies obtained are 3.24 and 3.09 eV for NiO and NiO/CoPc, respectively. The decrease in band gap for the composite is due to crystallite growth which results in the broadening of highest occupied molecular orbit in the valence band (HOMO) and the lowest unoccupied molecular orbit in the conduction band (LUMO) energy levels. The

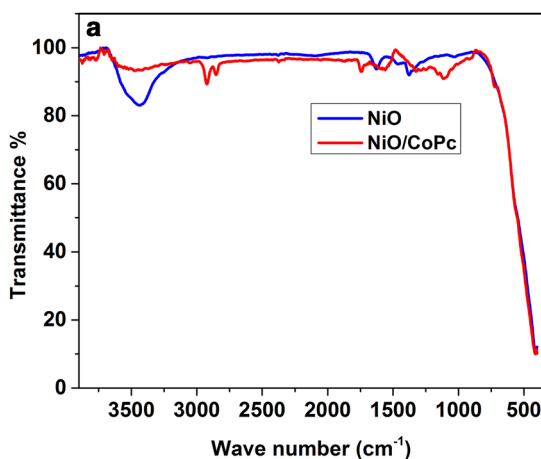


Fig. 6 FTIR spectra of a NiO and b NiO/CoPc nanocomposite

Table 2 Comparison of Infrared active modes of NiO and NiO/CoPc nanocomposite

Samples		Literature values	Band assignments
NiO	NiO/CoPc	CoPc [21]	
410	414	–	Ni–O stretching vibration
	723	721	C–H out of plane deformation (α phase)
	918	911	Metal ligand vibration
	1112	1117	C–H in plane bending
	1156	1162	C–N in plane bending
	1287	1287	C–N stretching in isoindole
	1330	1329	C–C stretching in isoindole

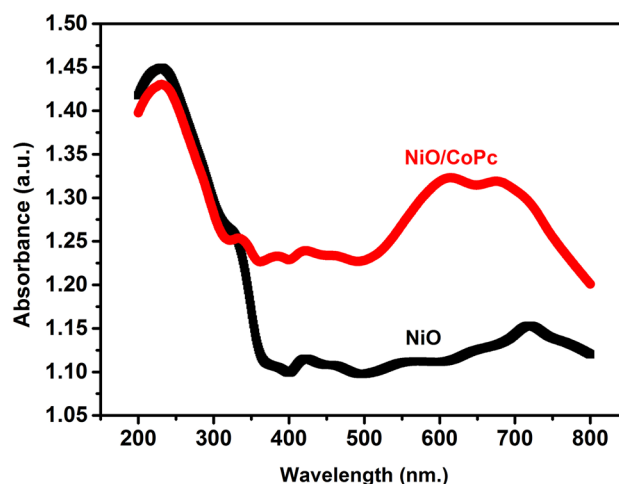
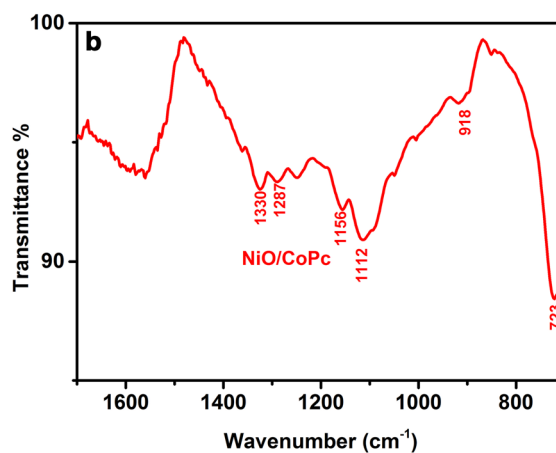


Fig. 7 Absorption spectra of NiO and NiO/CoPc nanocomposite

addition of CoPc into NiO has extended the absorption from UV to visible region of NiO, suggesting visible light photocatalytic application of the nanocomposite.



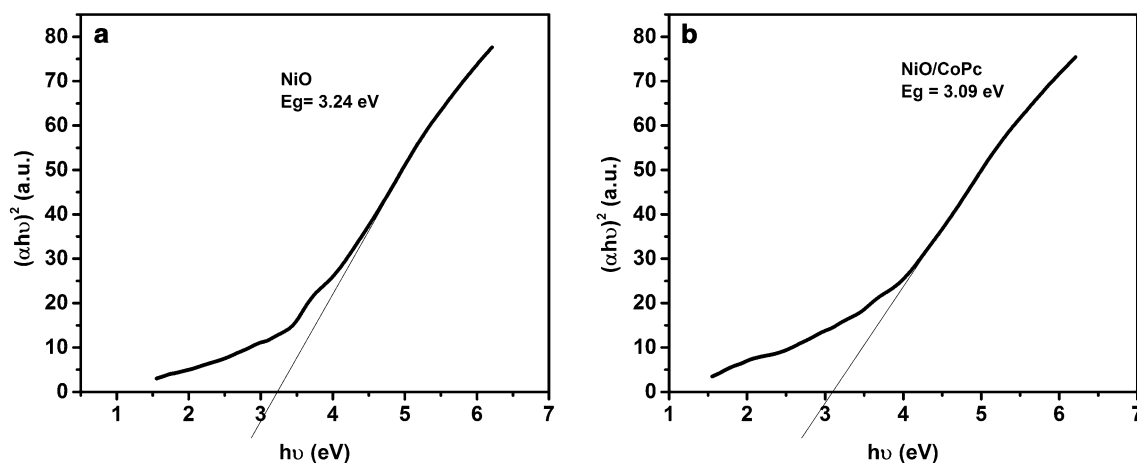


Fig. 8 $h\nu$ vs. $(\alpha h\nu)^2$ plot of **a** NiO and **b** NiO/CoPc nanocomposite

PL studies

Room temperature photo luminescence spectra ($\lambda_{\text{ex}} = 280$ nm) for NiO and NiO/CoPc are shown in Fig. 9. There is a broad emission band ranging from 325 to 425 nm with a peak located at 395 nm. This corresponds to the emission of free and bound excitons produced by oxygen vacancies and surface defects of NiO. Several shoulder peaks at 314, 447, 463, 479 and 489 nm in the violet–blue region are also observed for both the samples. The shape of the PL spectra of the composite is similar to that of NiO indicating that the inclusion of CoPc does not cause new fluorescent phenomena because of strong spin–orbit interaction [28]. As the surface oxygen vacancies of NiO can bind electrons to form excitons, the fluorescent effects of the composites are caused by the surface structure of NiO.

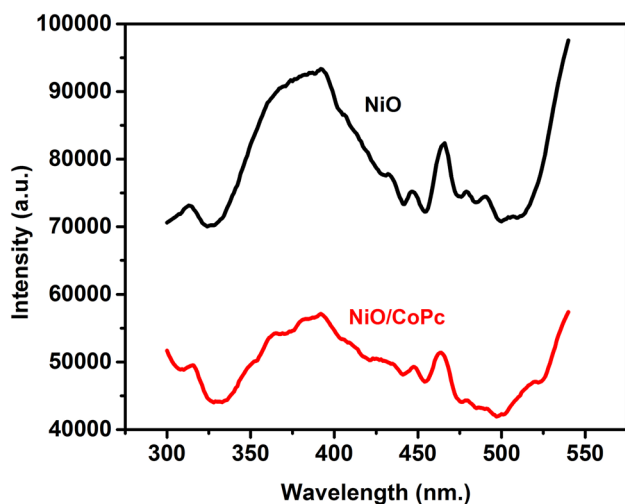


Fig. 9 PL spectra of NiO and NiO/CoPc nanocomposites

The efficiency of electron trapping and recombination of electrons and holes determines the emission peak intensity. Compared to pure NiO, PL spectrum of the composite suffers a reduction in intensity. This emission quenching represents the interaction and electron transfer process between CoPc and NiO. The result indicates that the composite can effectively block the electron–hole recombination in NiO, and improve the efficiency of separation of electrons and holes [29]. This will in turn enhance the photocatalytic activity of the composite. Hence, the photo-efficiency and photo-activity of NiO nanoparticles can be improved with the addition of CoPc of appropriate concentration which makes them suitable for potential applications in solar cells and photocatalysis.

Conclusion

NiO/CoPc nanocomposite is synthesized by simple solvent evaporation method. TGA/DTG studies confirm the thermal stability of the sample. The formation of NiO/CoPc nanocomposite is confirmed by the XRD, TEM and FTIR results. UV–visible absorption studies indicate a decrease in band gap energy along with an enhanced and extended visible light absorption for the nanocomposite. The emission quenching in PL spectrum makes them suitable for solar cells and photocatalysis and for potential applications in varied fields.

Acknowledgements The authors acknowledge Nirmala College, Muvattupuzha and Newman College, Thodupuzha for providing the facilities to conduct this study. They are also grateful to SAIF Cochin and Maharajas College, Ernakulam for the technical support rendered. The first author acknowledges the University Grants Commission for facilitating the research work through FDP.



Open Access This article is distributed under the terms of the Creative Commons Attribution 4.0 International License (<http://creativecommons.org/licenses/by/4.0/>), which permits unrestricted use, distribution, and reproduction in any medium, provided you give appropriate credit to the original author(s) and the source, provide a link to the Creative Commons license, and indicate if changes were made.

References

- Anees, A.A., Khan, M.A.M., Naziruddin, K.M., Salman, A.A., Alhoshan, M., Alsahhi, M.S.: Optical and electrical properties of electrochemically deposited polyaniline/CeO₂ hybrid nanocomposite film. *J. Semicond.* **32**, 043001–043006 (2011)
- Leznoff, C.C., Lever, A.B.P.: *Phthalocyanines: properties and applications*. Wiley, New York (1989)
- Saravanan, S., Joseph Mathai, C., Anantharaman, M.R., Venkatachalam, S., Prabhakaran, P.V.: Dielectric and conductivity studies on cobalt phthalocyanine tetramers. *J. Appl. Polym. Sci.* **9**, 2529–2535 (2004)
- Yuen, A.P., Jovanovic, S.M., Hor, A., Klenkler, R.A., Devenyi, G.A., Loutfy, R.O., Preston, J.S.: Photovoltaic properties of *M*-phthalocyanine/fullerene organic solar cells. *Sol. Energy* **86**, 1683–1688 (2012)
- Zhang, X., Lin, Y., Guo, W., Zhu, J.: Spectroscopic insights on imidazole substituted phthalocyanine photosensitizers: fluorescence properties, triplet state and singlet oxygen generation. *Spectrochim. Acta Part A Mol. Biomol. Spectrosc.* **133**, 752–758 (2014)
- Wang, Y., Dejian Liang, D.: Solvent-stabilized photoconductive metal phthalocyanine nanoparticles: preparation and application in single-layered photoreceptors nanoparticles: preparation and application in single-layered photoreceptors. *Adv. Mater.* **22**, 1521–1525 (2010)
- Öztürk, Z.Z., Kılınc, N., Atilla, D., Gürek, A.G., Ahsen, V.: Recent studies chemical sensors based on phthalocyanines. *J. Porphy. Phthalocyanines* **13**, 1179–1187 (2009)
- Xie, D., Jiang, Y., Pan, W., Jiang, J., Wu, Z., Li, Y.: The characteristics and gas-sensing property of bis[phthalocyaninato] rare earth complexes based charge-flow transistor. *Sens. Actuators B* **81**, 210–217 (2002)
- Mathews, S.J., Chaitanya Kumar, S., Giribabu, L., Venugopal Rao, S.: Nonlinear optical and optical limiting properties of phthalocyanines in solution and thin films of PMMA at 633 nm studied using a cw laser. *Mater. Lett.* **61**, 4426–4431 (2007)
- Madhu, G., Bose, V.C., Aiswaryaraj, A.S., Maniammal, K., Biju, V.: Defect dependent antioxidant activity of nanostructured nickel oxide synthesized through a novel chemical method. *Colloids Surf. A Physicochem. Eng. Asp.* **429**, 44–50 (2013)
- Priyanka, K.P., Sankararaman, S., Balakrishna, K.M., Varghese, T.: Enhanced visible light photocatalysis using TiO₂/phthalocyanine nanocomposites for the degradation of selected industrial dyes. *J. Alloys Compd.* **720**, 541–549 (2017)
- Liu, S., Zhao, Z., Wang, Z.: Photocatalytic reduction of carbon dioxide using sol–gel derived titania-supported CoPc catalysts. *Photochem. Photobiol. Sci.* **6**, 695–700 (2007)
- Babitha, K.K., Priyanka, K.P., Sreedevi, A., Jaseentha, O.P., Varghese, T.: Structural modifications and extended spectral response of CeO₂/CoPc nanocomposites for potential applications. *Int. J. Appl. Ceram. Technol.* **13**, 670–677 (2016)
- Sheena, P.A., Priyanka, K.P., Aloysius Sabu, N., Sabu, B., Varghese, T.: Effect of calcination temperature on the structural and optical properties of nickel oxide nanoparticles. *Nanosyst. Phys. Chem. Math.* **5**, 441–449 (2014)
- Borker, P., Salker, A.V.: Synthesis, characterization and photocatalytic studies of some metal phthalocyanines. *Indian J. Chem. Technol.* **13**, 341–346 (2006)
- Burgos, F.V., Utsumi, S., Hattori, Y., et al.: Pyrolyzed phthalocyanines as surrogate carbon catalysts: initial insights into oxygen-transfer mechanisms. *Fuel* **99**, 106–117 (2012)
- Cullity, B.D.: *Elements of X-Ray Diffraction*. Addison-Wesley, Reading (1967)
- Williamson, G.K., Hall, W.H.: X-ray line broadening from filed aluminum and wolfram. *Acta Metall.* **1**, 22–31 (1953)
- Anandan, K., Rajendran, V.: Morphological and size effects of NiO nanoparticles via solvothermal process and their optical properties. *Mater. Sci. Semicond. Process.* **14**, 43–47 (2011)
- Sheena, P.A., Priyanka, K.P., Sabu, N.A., Gannesh, S., Varghese, T.: Effect of electron beam irradiation on the structure and optical properties of nickel oxide nanocubes. *Bull. Mater. Sci.* **38**, 825–830 (2015)
- Verma, D., Dash, R., Katti, K.S., Schulz, D.L., Caruso, A.N.: Role of coordinated metal ions on the orientation of phthalocyanine based coatings. *Spectrochim. Acta Part A* **70**, 1180–1186 (2008)
- Li, X., Zhang, X., Li, Z., Qian, Y.: Synthesis and characteristics of NiO nanoparticles by thermal decomposition of nickel dimethylglyoximate rods. *Solid State Commun.* **137**, 581–584 (2006)
- Manna, S., Deb, A.K., Jagannanth, J., De, S.K.: Synthesis and room temperature ferromagnetism in Fe doped NiO nanorods. *J. Phys. Chem. C* **112**, 10659–10662 (2008)
- Rajesh, K.R., Menon, C.S.: Electrical and optical properties of vacuum deposited ZnPc and CoPc thin films and application of variable range hopping model. *Indian J. Pure Appl. Phys.* **43**, 964–971 (2005)
- Seoudi, R., El-Bahy, G.S., El Sayed, Z.A.: Ultraviolet and visible spectroscopic studies of the phthalocyanine and its complexes thin films. *Opt. Mater.* **29**, 304–312 (2006)
- Sreedevi, A., Priyanka, K.P., Babitha, K.K., Jaseentha, O.P., Varghese, T.: Structural and optical modifications of the Ag₂WO₄/CoPc nanocomposite for potential applications. *Eur. Phys. J. Plus* **131**, 1–7 (2016)
- Joseph, B., Menon, C.S.: Studies on the optical properties and surface morphology of cobalt Phthalocyanine thin films. *J. Chem.* **5**, 86–92 (2008)
- Bała, W., Wojdyła, M., Rębarz, M., Szybowic, M., Drozdowski, M., Grodzicki, A., Piszczek, P.: Influence of central metal atom in MPc (M=Cu, Zn, Mg, Co) on Raman, FT-IR, absorbance, reflectance, and photoluminescence spectra. *J. Optoelectron. Adv. Mater.* **11**, 264–269 (2009)
- Gu, L., Wang, J., Cheng, H., Zhao, Y., Liu, L., Han, X.: One-step preparation of graphene-supported anatase TiO₂ with exposed 001 facets and mechanism of enhanced photocatalytic properties. *ACS Appl. Mater. Interfaces.* **5**, 3085–3093 (2013)

Publisher's Note Springer Nature remains neutral with regard to jurisdictional claims in published maps and institutional affiliations.

Affiliations

P. A. Sheena^{1,2} · K. P. Priyanka³ · A. Sreedevi³ · Thomas Varghese³

¹ Department of Physics, M.E.S. Asmabi College,
Kodungallur, Padinjare Vemballur, Kerala 680 671, India

² Department of Physics, Newman College, Thodupuzha,
Kerala 685584, India

³ Department of Physics, Nanoscience Research Centre
(NSRC), Nirmala College, Muvattupuzha, Kerala 686661,
India

